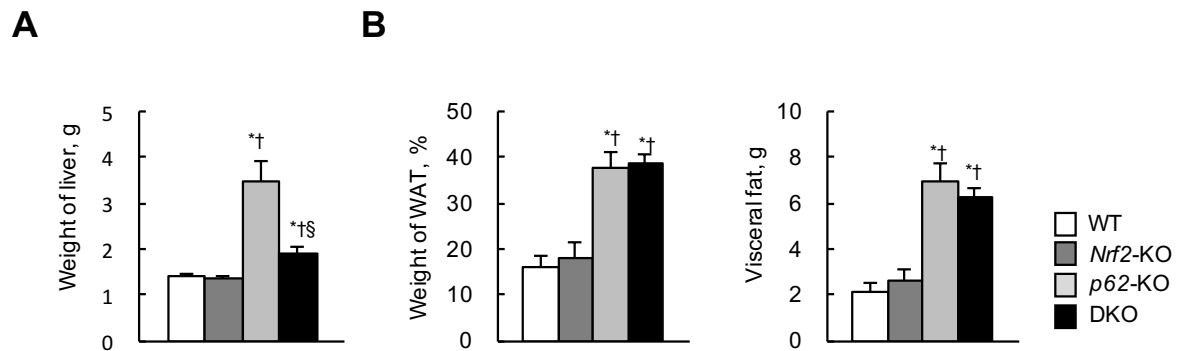


## Supplementary File

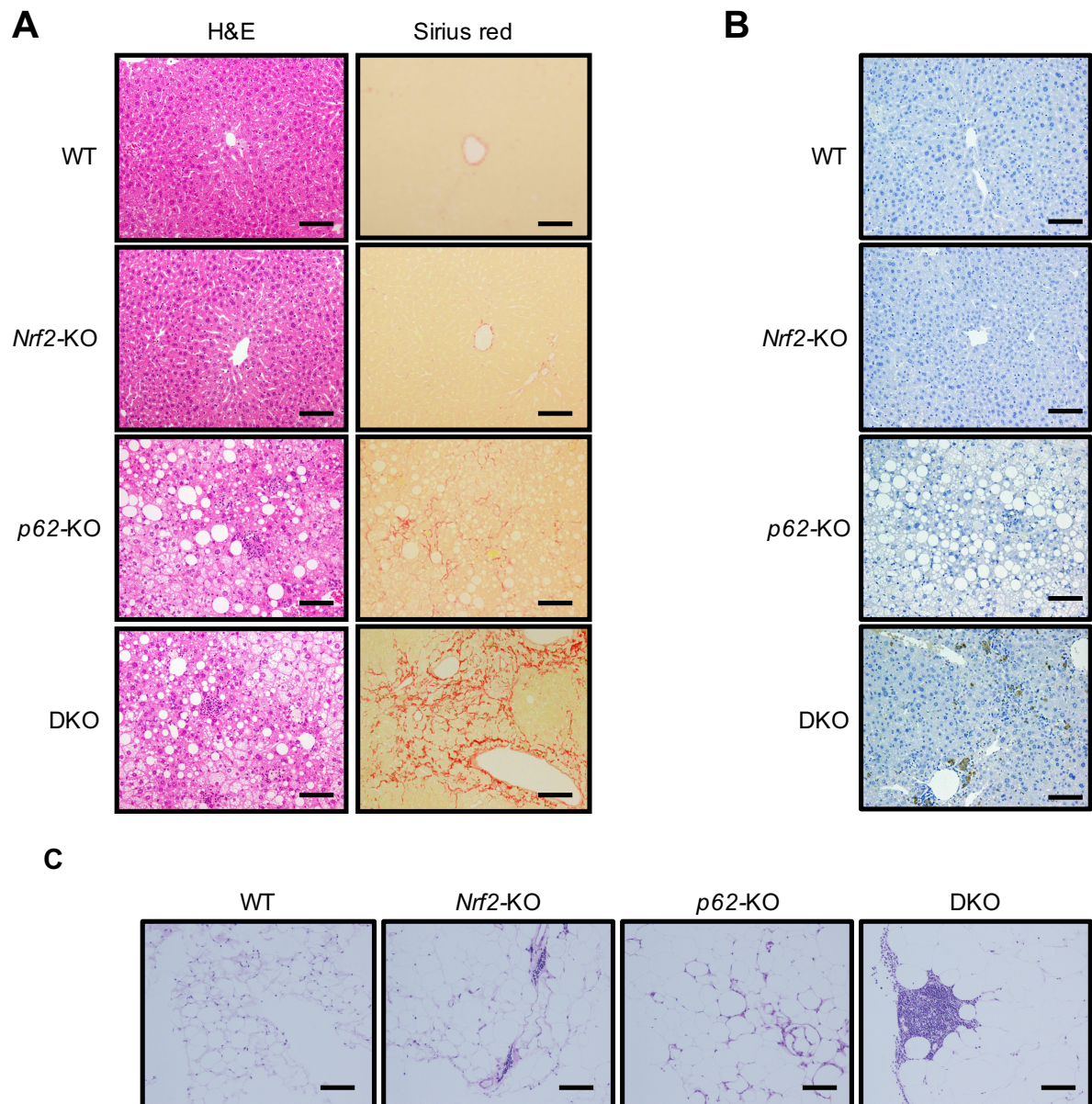
### Supplementary Figure 1



### Supplementary Figure 1.

*p62:Nrf2* double-knockout (DKO) mice exhibited increased liver mass, visceral fat accumulation, and obesity. **(A)** Liver mass in wild-type (WT), *Nrf2*-knockout (KO), *p62*-KO, and DKO mice at 30 weeks of age ( $n = 8$  per group). **(B)** Computed tomography (CT) analysis of the weight of white adipose tissue (WAT) and visceral fat content in WT, *Nrf2*-KO, *p62*-KO, and DKO mice at 30 weeks of age ( $n = 8$  per group). For CT analysis of body fat composition, mice were anesthetized with isoflurane and scanned using a Latheta micro-CT scanner (LCT-200, Hitachi Aloka Medical, Tokyo, Japan). Results are presented as the mean  $\pm$  SE. Statistical significance was determined using ANOVA with Scheffé's multiple testing correction. \* $P < 0.05$ , significantly different from the WT group; † $P < 0.05$ , significantly different from the *Nrf2*-KO group; § $P < 0.05$ , significantly different from the *p62*-KO group.

## Supplementary Figure 2

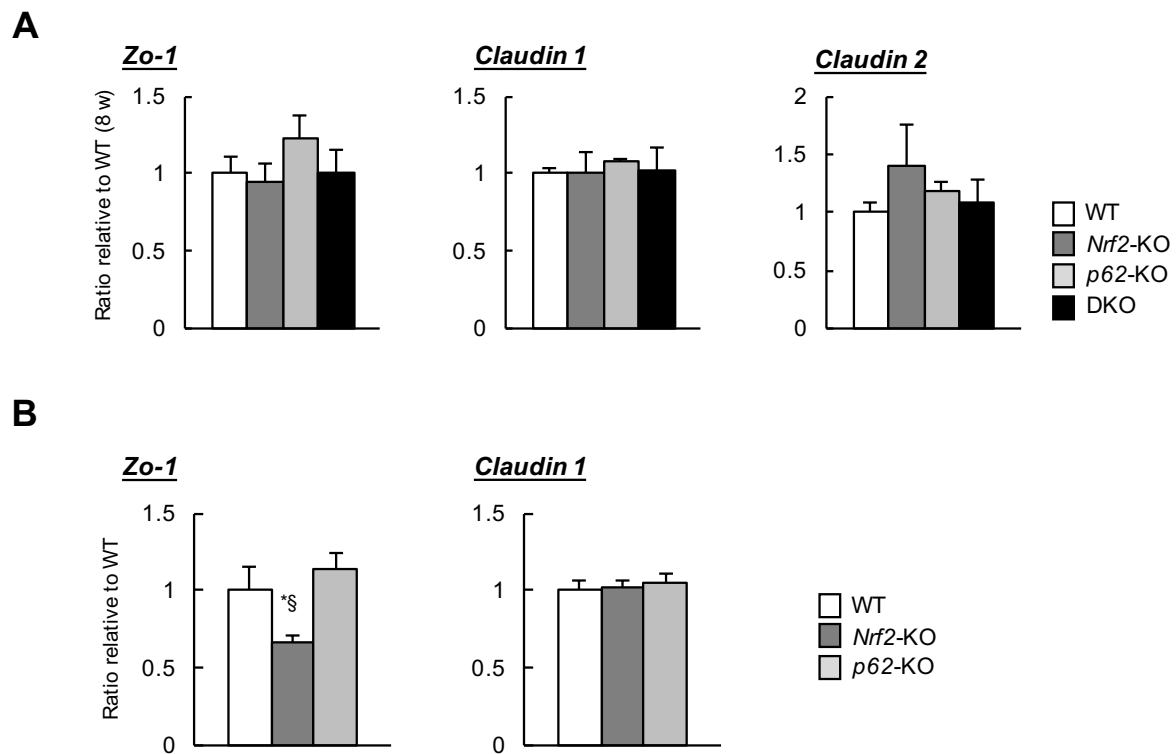


## Supplementary Figure 2.

*p62:Nrf2* double-knockout (DKO) mice exhibited severe inflammation in the liver and visceral fat tissue with aging. **(A)** Hematoxylin and eosin (H&E)-stained and sirius red-stained sections of representative liver specimens from wild-type (WT), *Nrf2*-knockout (KO), *p62*-KO, and DKO mice at 50 weeks of age (scale bar, 100  $\mu$ m). **(B)** Immunostaining

with 4-hydroxy-2-nonenal (4-HNE) was performed to determine the presence of lipid peroxides (scale bar, 100  $\mu\text{m}$ ). **(C)** H&E-stained sections of representative visceral fat tissue specimens at 30 weeks of age (scale bar, 100  $\mu\text{m}$ ).

### Supplementary Figure 3



### Supplementary Figure 3.

Deficiency of Nrf2 in Caco-2 cells reduced the expression of *Zo-1* of tight junction proteins.

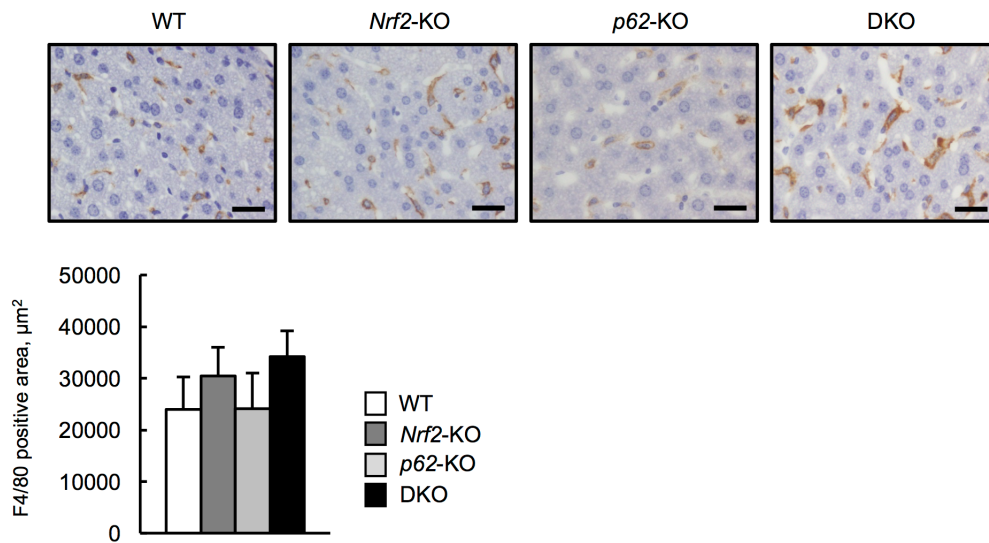
**(A)** Relative expression levels of intestine zona occludens-1 (*Zo-1*), *claudin 1*, and *claudin 2* mRNA in wild-type (WT), *Nrf2*-knockout (KO), *p62*-KO, and DKO mice at 8 weeks of age (n = 8 per group).

**(B)** Relative expression levels of *Zo-1* and *claudin 1* mRNA in WT, *Nrf2*-KO, and *p62*-KO Caco-2 cells (n = 5 per group). mRNA expression levels were calculated as the ratio relative to that in WT. Results are presented as the mean  $\pm$  SE.

Statistical significance was determined using ANOVA with Scheffé's multiple testing correction. \* $P < 0.05$ , significantly different from the WT group;  $^{\dagger}P < 0.05$ , significantly different from the *Nrf2*-KO group;  $^{\S}P < 0.05$ , significantly different from the *p62*-KO group.



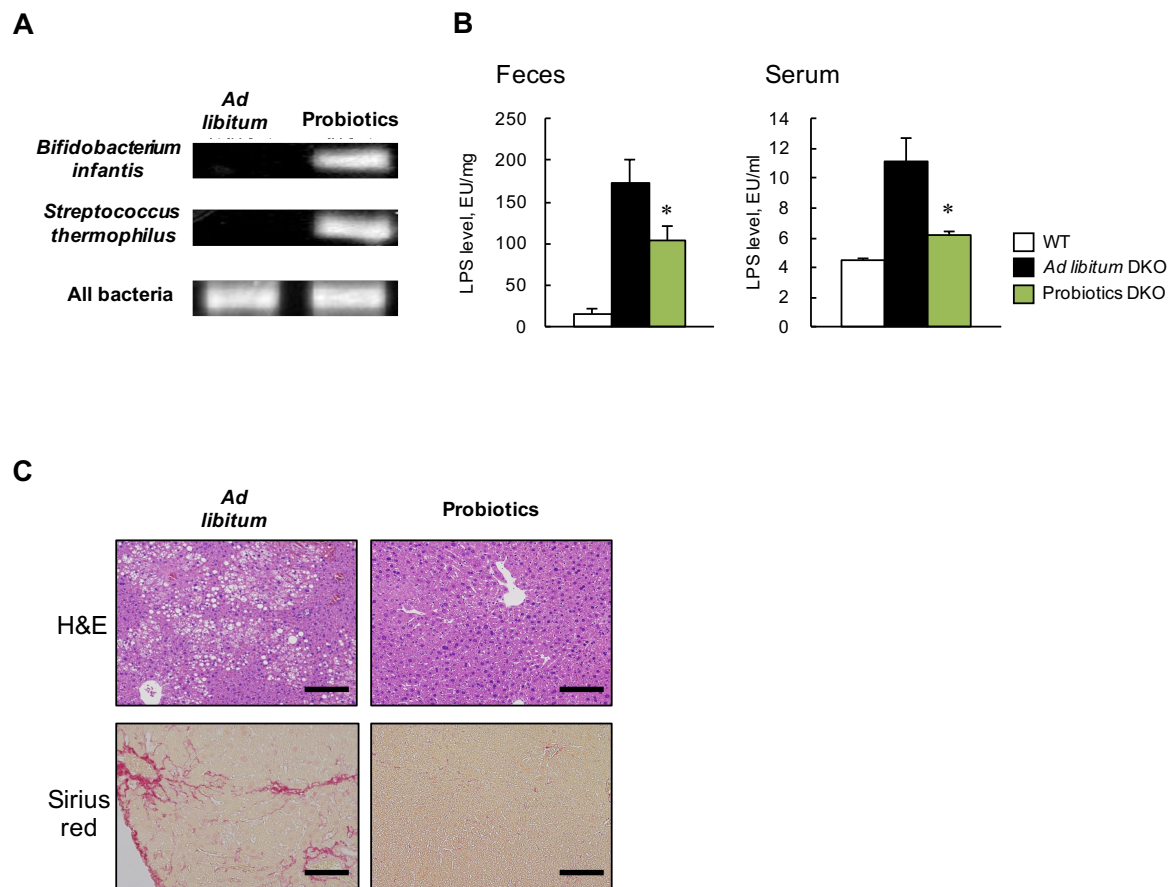
## Supplementary Figure 4



### Supplementary Figure 4.

The number of Kupffer cells in *p62:Nrf2* double-knockout (DKO) mice did not change at 8 weeks of age. Immunostaining with F4/80 was performed to determine the presence of Kupffer cells (scale bar, 50  $\mu\text{m}$ ). F4/80-positive areas in the livers of wild-type (WT), *Nrf2*-knockout (KO), *p62*-KO, and DKO mice ( $n = 8$  per group). Results are presented as the mean  $\pm$  SE. Statistical significance was determined using ANOVA with Scheffé's multiple testing correction. \* $P < 0.05$ , significantly different from the WT group;  $^{\dagger}P < 0.05$ , significantly different from the *Nrf2*-KO group;  $^{\S}P < 0.05$ , significantly different from the *p62*-KO group.

## Supplementary Figure 5



## Supplementary Figure 5.

Probiotics improved nonalcoholic steatohepatitis (NASH) in *p62:Nrf2* gene double-knockout (DKO) mice. **(A)** PCR of *Bifidobacterium infantis* and *Streptococcus thermophilus* in feces. **(B)** Fecal and serum lipopolysaccharide (LPS) levels in WT, *ad libitum* DKO, and probiotics mice (n = 8 per group). **(C)** Hematoxylin and eosin (H&E)- and sirius red-stained sections of representative liver specimens from the *ad libitum* DKO and probiotics groups at 25 weeks of age (scale bar, 100  $\mu$ m). Results are presented at the mean  $\pm$  SE. Statistical significance was determined using ANOVA with Scheffé's multiple testing correction. \* $P$ <0.05, significantly different from the *ad libitum* DKO group.

**Supplementary Table 1. Antibodies for immunoblotting, immunohistochemistry, and flow cytometry.**

Antibodies	Manufacturer	Cat No.
Rabbit polyclonal anti-p62	Ishii et al., 2000	N/A
Rabbit polyclonal anti-Nrf2	Proteintech	16396-1-AP
Rabbit polyclonal anti-actin	Sigma-Aldrich	A5060
Rabbit polyclonal anti-Lamin A/C	Cell Signaling Technology	2032
Rabbit monoclonal anti-NF- $\kappa$ B p65 phospho	Cell Signaling Technology	3033
Rabbit monoclonal anti-NF- $\kappa$ B p65	Cell Signaling Technology	4764
Rabbit polyclonal anti-Keap1	Cell Signaling Technology	4617S
Rabbit polyclonal anti-Zo-1	Thermo Fisher Scientific	61-7300
Mouse monoclonal anti-claudin 1	Thermo Fisher Scientific	37-4900
Mouse monoclonal anti-claudin 2	Thermo Fisher Scientific	32-5600
Mouse monoclonal anti-4-hydroxy-2-nonenal	JaiCA	MHN-100P
Rabbit polyclonal anti-glutathione S-transferase P1	MBL	311
Sheep anti-mouse IgG, HRP-linked whole Ab	GE Healthcare	NA931
Donkey anti-rabbit IgG, HRP-linked whole Ab	GE Healthcare	NA934
Rat monoclonal APC-conjugated anti-F4/80	Thermo Fisher Scientific	17-4801-82
PerCP/Cy5.5 anti-mouse CD206	BioLegend	141715
PE anti-mouse CD11c	BioLegend	117307
Rat monoclonal anti-mouse MARCO	BIO-RAD	MCA1849
Goat polyclonal anti-mouse SR-A1	R&D Systems	AF1797
Goat anti-rat IgG, Alexa Fluor 488	Thermo Fisher Scientific	A-11006
Donkey anti-goat IgG, Alexa Fluor 488	Thermo Fisher Scientific	A-11055

**Supplementary Table 2. Primers for real-time PCR analysis.**

Genes	Primer sequences (5' - 3')	
	Forward	Reverse
<i>Tnf-α</i>	AAGCCTGTAGCCCACGTCGTA	GGCACCAGTAGTTGGTTGTCTTTG
<i>Il-1β</i>	TCCAGGATGAGGACATGAGCAC	GAACGTCACACACCAGCAGGTTA
<i>Il-6</i>	GAGGATACTACTCCCAACAGACC	AAGTGCATCATCGTTGTTTCATACA
<i>Tlr-4</i>	GCAGCAGGTGGAATTGTATCG	TGTGCCTCCCCAGAGGATT
<i>Tgf-β1</i>	GTGTGGAGCAACATGTGGAAGTCTA	TTGGTTCAGCCACTGCCGTA
<i>Procollagen-α1</i>	GCACGAGTCACACCGGAAGT	AAGGGAGCCACATCGATGAT
<i>Mcp-1</i>	TTCCTCCACCACCATGCAG	CCAGCCGGCAACTGTGA
<i>Cd14</i>	CCTGCCCTCTCCACCTTAGAC	TCAGTCCTCTCTCGCCCAAT
<i>Zo-1</i>	GCTAAGAGCACAGCAATGGA	GCATGTTCAACGTTATCCAT
<i>Claudin 1</i>	CGGGCAGATACAGTGCAAAG	ACTTCATGCCAATGGTGGAC
<i>Claudin 2</i>	CAACTGGTGGGCTACATCCTA	CCCTTGGAAGGCAACCG
<i>Zo-1</i> (human)	GAATGATGGTTGGTATGGTGCG	TCAGAAGTGTGTCTACTGTCCG
<i>Claudin1</i> (human)	GCACATACCTTCATGTGGCTCAG	TGGAACAGAGCACAAACATGTCA

Tnf, tumor necrosis factor; Il, interleukin; Tlr, toll-like receptor; Mcp, monocyte chemotactic protein; Cd, cluster of differentiation; Tgf, transforming growth factor; Zo, zona occludens.

**Supplementary Table 3. The RNA-guided CRISPR Cas9 system.**

Cells	Genes	Sequences (5' - 3')
RAW264.7	<i>Nrf2</i>	GATGTGCTGGGCCGGCTGAAT
	<i>p62</i>	GTTGGGGTGCACCATGTTTCG
Caco-2	<i>Nrf2</i>	GCGACGGAAAGAGTATGAGC
	<i>p62</i>	GAGCCATCGCAGATCACATTG